Journal of Natural Gas Science and Engineering 50 (2018) 33–42

Contents lists available at ScienceDirect

Journal of Natural Gas Science and Engineering

journal homepage: www.elsevier.com/locate/jngse

Shale oil and gas resources in organic pores of the Devonian Duvernay Shale, Western Canada Sedimentary Basin based on petroleum system modeling

Pengwei Wang[a,b], Zhuoheng Chen[b], Zhijun Jin[a], Chunqing Jiang[b], Mingliang Sun[b,c], Yingchun Guo[d,*], Xiao Chen[e], Zekai Jia[b]

[a] Research Institute of Petroleum Exploration & Production, SINOPEC, Beijing 100083, China
[b] Geological Survey of Canada, Calgary T2L 2A7, Canada
[c] Basin and Reservoir Research Center, College of Geosciences, China University of Petroleum, Beijing 102249, China
[d] Institute of Geomechanics, Chinese Academy of Geological Sciences, Beijing 100081, China
[e] CNOOC Research Institute, Beijing 100028, China

ARTICLE INFO

Keywords:
Petroleum system modeling
Organic porosity
Adsorbed gas
Shale oil and gas resources
Duvernay Shale
Western Canada Sedimentary Basin

ABSTRACT

Shale-hosted hydrocarbons is regarded as an important unconventional resource around the world. So far, huge emphasis has been put on the contribution of organic pores to self-source and self-reservoir hydrocarbon systems. This study systemically reveals the contribution of organic pores to hydrocarbon potential in the Duvernay Shale through restoring thermal maturity evolution, modeling hydrocarbon generation and expulsion in the Duvernay Formation, analyzing absorption capacity variation with TOC and modeled pore pressure, determining free-gas storage capacity with calculated organic porosity and correction of adsorbed gas, and calculating in-place shale oil and gas volumes with volumetric method. The Duvernay Shale reached "oil window" and "gas window" about 70–80 Ma and 50 Ma ago, respectively. Significant hydrocarbon generation (20% TR) began and terminated (95% TR) at Ro of 0.65% and 1.85%, respectively. Gas generation rates increased dramatically from Ro of 1.1%, while the instantaneous HC_{1-4} expulsion reached peak at Ro of 1.66%, the difference between which indicates considerable retained gas resource in Duvernay Shale. The gas storage capacity, including absorption capacity and free gas capacity, varies significantly in the Duvernay Shale, specifically, the former rangs from 8 to 30scf/ton, and the latter from 40 to 140scf/ton. The estimated median value of total in-place natural gas (GIP) and in-place oil resource (OIP) in organic pores of Duvernay shale are 404.8 TCF and 81420 MMbbl, respectively. Thus, the organic porosity is one of the keys to make the Duvernay Shale a successful play.

1. Introduction

The Duvernay Formation, part of the Upper Devonian Woodbend Group in the West Canada Sedimentary Basin (WCSB), has been recognized as an important source rock, which generated and expelled large amount hydrocarbon to the conventional fields, such as the prolific Leduc oil and Swan Hills gas reservoirs in the overlain Devonian carbonate reefs and platform carbonates (Stoakes and Creaney, 1984). Currently, industrial data from recent pilot production wells prove that the Devonian Duvernay Formation is one of the most potential hydrocarbon-rich shale plays in WCSB.

Considerable studies have proved that nano-metre scale pores occurred in organic matter in organic-rich shale (Anderson et al., 2010; Modica and Lapierre, 2012; Dunn et al., 2012; Lu et al., 2015; Chen and Jiang, 2016). For example, SEM images from a series of organic-rich and mature core samples of the Duvernay Formation provide visual support for the belief that organic pores exist in shale with the maximum porosity up to 6% in high mature samples (Chen and Jiang, 2016). Previous works have been performed on samples from various basins to understand how organic pores developed in the organic matter of shales as well as the controlling factors (Loucks et al., 2009, 2011, 2012; Modica and Lapierre, 2012; Chalmers et al., 2012; Curtis et al., 2012; Curtis, 2013; Romero-Sarmiento et al., 2014; Lu et al., 2015; Pommer and Milliken, 2015; Chen and Jiang, 2016). Generally, nano-metre scale pores occur in organic matter as a result of thermal decomposition of kerogen in organic-rich shale, increasing with thermal maturation (Anderson et al., 2010; Dunn et al., 2012; Modica and Lapierre, 2012; Chen and Jiang, 2016). However, less effort was made to describe systematically the hydrocarbon resource potential hosted by organic pores, especially the spatial variation of free gas capacity and absorption capacity.

Petroleum system modeling has been long regarded as a valuable

* Corresponding author.
E-mail address: lansefengye315@126.com (Y. Guo).

https://doi.org/10.1016/j.jngse.2017.10.027
Received 20 June 2017; Received in revised form 30 October 2017; Accepted 31 October 2017
Available online 02 December 2017
1875-5100/

tool for conventional play analysis, e.g., simulating hydrocarbon generation and charging process to determine the volume of hydrocarbons available for entrapment, modeling fluid flow to predict the volumes and locations of hydrocarbon accumulations (Romero-Sarmiento et al., 2013). In terms of unconventional resources system, especially self-contained source-reservoir shale system, petroleum system modeling is a useful tool to describe source rocks, e.g., kerogen kinetics, burial history and thermal history, as well as hydrocarbon generation and expulsion history. However, so far, traditional petroleum system modeling methods can't be used to evaluate shale reservoir quality and investigate hydrocarbon retention mechanisms, such as describing and characterizing pore systems as well as their generation and evolution (Pommer and Milliken, 2015; Ko et al., 2016), determining free gas capacity and adsorption capacity, etc. (Ross and Bustin, 2007; Loucks et al., 2009; Zhang et al., 2012).

Thus, this study examined the hydrocarbon resource potential in organic pores of the Duvernay Shale using petroleum system modeling method. Hydrocarbon generation and expulsion were revealed by thermal history and kerogen kinetics modeling. Organic porosity in shales as well as its spatial variations were determined with modeled kerogen kinetics and geochemical data (Chen and Jiang, 2016). Free gas capacity and absorption capacity in those organic pores as well as their spatial variations were determined, based on which the oil and gas resources potential were estimated through volumetric method. Since a significant portion of hydrocarbons occur as adsorbed gas that occupies part of the pore space in source rock reservoir, a correction of the amount of adsorbed gas was performed to eliminate the impact of its occupation of pore space on free gas estimation.

2. Geological setting

The Duvernay Shale was deposited uniquely as the basin time equivalent of Leduc reef growth during the Frasnian age (Fig. 1) (Stoakes and Creaney, 1984; Allan and Creaney, 1991; Chow et al., 1995; Stasiuk and Fowler, 2002, 2004). Since repaid depositing during the maximum transgressive period of the Woodbend, the Duvernay Shale represents an enormous succession of oxygen-starved accumulation and preservation of organic carbons. Five lithofacies have been identified from the Duvernay Formation, including argillaceous mudstones, bioturbated limestone, siliceous organic rich mudstones, mixed siliceous mudstone and limestone (Dunn et al., 2012), while argillaceous mudstones and siliceous organic rich mudstones were defined as the hydrocarbon source rocks in Duvernay Shale (Stasiuk and Fowler, 2004).

The rapid basin-fill at maximum sea-level transgression deposited large quantities of organic sediments, resulting in a high total organic carbon (TOC) content of 6–20%. Being characterized by type II kerogen, the Duvernay Shale exhibits increased thermal maturity to the west, and about 15% of the source rock is within “gas window” in the central Alberta (Rokosh et al., 2012).

The WCSB experienced two periods of erosion. Specifically, the first erosion corresponding to the Sub-Mannville Unconformity was assumed to occur from 150Ma to 119Ma with minimal loss of strata. The second erosion, the Laramide Orogeny (from 57.8 Ma to the present), is the critical event with the estimated erosion thickness ranging from 1600 to 2000m along the west of the deformed belt to 400–600 m in the northeast of study area (Higley et al., 2009).

SEM image in Fig. 2A shows organic pore networks in organic-rich shale core samples from the Duvernay Formation. As the organic matters (OM) uniformly fill the intergranular spaces of minerals, nanometre-size organic pores are the most abundant pore type observed in the investigated samples (Fig. 2A). Fig. 2B is an image of Helium Ion Microscopy (HIM) showing the topographic feature of the organic pores within organic matter. The diameters of organic pores in these two shale images range from a few nanometers to close to a hundred nanometers. The presence of a large volume of nano-pores associated with

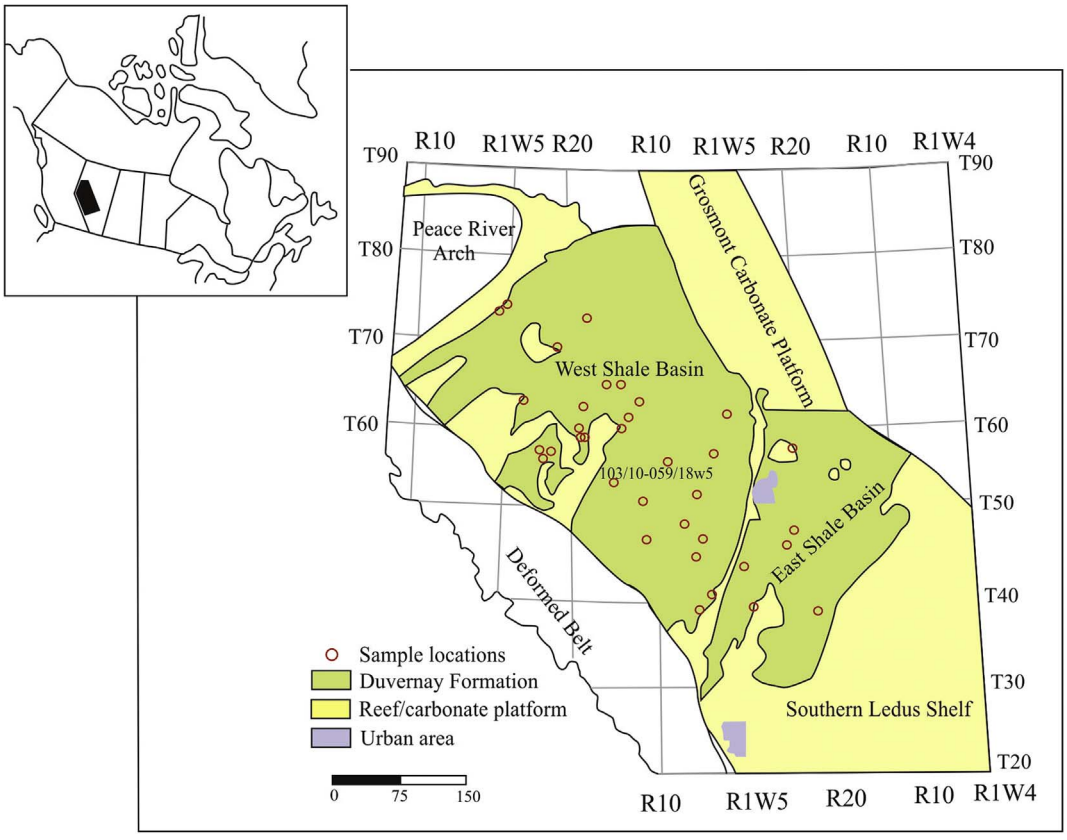

Fig. 1. Map showing the study area with generalized geological setting in the Western Canada Sedimentary Basin (Rokosh et al., 2012).

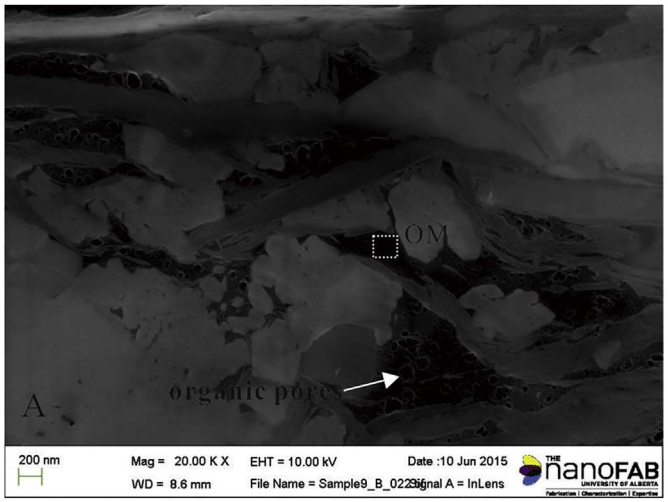

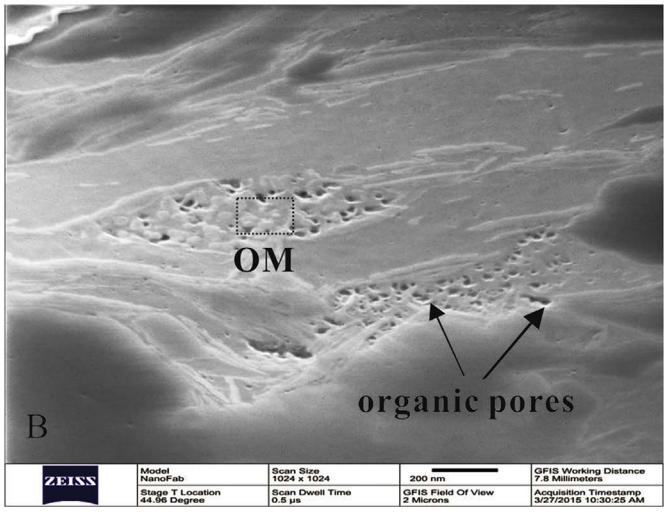

Fig. 2. Scanning electron microscope (SEM) image shows the organic pores in the Duvernay Formation. OM and organic pores have been labelled with square frame and arrows, respectively. Organic pores are irregular in shape, variable in size and concentrate in certain part of OM (08-15-62-18W5 Well, depth: 3016.3 m, Tmax = 460 °C; Ro = 1.29%) (A). HIM image of core sample of Duvernay Shale showing organic pores and their association with clay minerals (15-33-41-08W5 well, depth: 3454.2 m, Tmax: 473 °C; Ro = 1.35%) (B).

organic matters indicates the organic pores contribute significantly to hydrocarbon storage in the Duvernay Shale reservoir. The strong positive correlation between TOC and permeability (Fig. 3A) and permeability and porosity (Fig. 3B) in the Duvernay Shale suggest that kerogen decomposition contributed greatly to the growth of organic pores, which can provide considerable storage space and connected network in shale reservoir.

3. Data and method

3.1. Dataset

Three datasets are collected in this study, which include:

1) Stratigraphic dataset of regional structures, lithofacies, erosion and hiatus events.
2) Rock-Eval data describes the geochemical characteristic of the Duvernay Shale.
3) Calibration data from drilling and production, such as formation pressure and temperature, used for modelling geological process and correcting the modeled results.

3.1.1. Stratigraphy

The stratigraphic framework was built on the digital Atlas of Western Canada Sedimentary Basin by Mossop and Shetsen (1994). The 2-D model of the WCSB consists of 14 isopach layers representing intervals from the Middle Devonian Elk Point group (around 405 Ma) to the present with mentioned erosional events (Ducros et al., 2012). Layers stacked vertically on the top of the Elk Point Group based on the elevation. Vertical and lateral variations of lithology were assigned based on lithofacies variation from Mossop and Shetsen (1994). The second erosion event was considered in this paper, since it controlled hydrocarbon generation and expulsion in the Devonian source rocks, whereas the first event took place prior to the maximum burial depth with limited effects being expected on thermal maturation of underlying source rocks. Two hiatus events in WCSB were also included in the model, one in Pennsylvanian (from 345Ma to 339Ma) and the other in Permian (from 318Ma to 300Ma) respectively. Drilling data from 119 wells were used to correct the structure and formation thickness.

3.1.2. Rock-Eval data

A total of 315 core samples from 35 wells (Fig. 1) covering majority of the West Shale Basin were analyzed with Rock-Eval 6 instrument to establish kinetic model for determining organic porosity in the Duvernay Shale. Data screening was carried out to remove the impacts from organic-lean samples in the interbedded limestone beds as well as different kerogens type resulted from varied organic facies. A criterion of TOC values $>$ 1.5 wt% was used to eliminate poor quality data (Peters, 1986; Chow et al., 1995; Stasiuk and Fowler, 2004). Also, a trend of Tmax with increasing depth was used to remove the samples with anomalous Tmax values. As a result, only 215 reliable data was remained to describe the hydrocarbon generation and expulsion. The vitrinite reflectances (Ro) determined along measured Tmax from 35 wells were used to correct the spatial variation of thermal maturity in the Duvernay source rocks (Wust et al., 2013).

3.1.3. Calibration data

As mentioned, this study employed various data, including drilling, production and laboratory test data, to specifically govern the 2-D model and calibrate the simulation process.

The drill stem tests (DSTs) were collected from the Duvernay shale in WCSB, which indicates an abnormally high formation pressure in the reservoirs with the pressure gradients up to 20.3 kPa/m (Hammermaster et al., 2012; Low et al., 2013) (Fig. 4A).

A total of 164 temperature data from 338 wells was used to correct modeled temperature. Due to the negative impact from mud filtrate, about 30 unreliable data was removed. Fig. 4B illustrates the temperature variation with increasing depth in WCSB.

Hydrocarbon composition in the source rock is another type of important data for model calibration. The initial GOR of the Duvernay Shale from 47 wells was calculated from dividing the cumulative gas production (m^3) by the cumulative oil and condensate production (m^3) volumes in the first full month, with the values throughout the Duvernay Shale ranging from 0 to 2,837,200 scf/bbl (Fig. 5).

3.2. Method

The petroleum system modeling was conducted using Trinity 5.2, which integrated the geological history with hydrocarbon generation and expulsion to quantify critical parameters and provided a cost effective, all-purpose interactive map-based petroleum system analysis. The properties of source rocks, e.g., burial history and thermal history, kerogen kinetics were reconstructed to describe oil/gas generation and expulsion process, and consequently, current thermal maturity and pore pressure as well as their spatial variations of the Duvernay Shale were modeled to determine gas capacity with following analysis. The organic

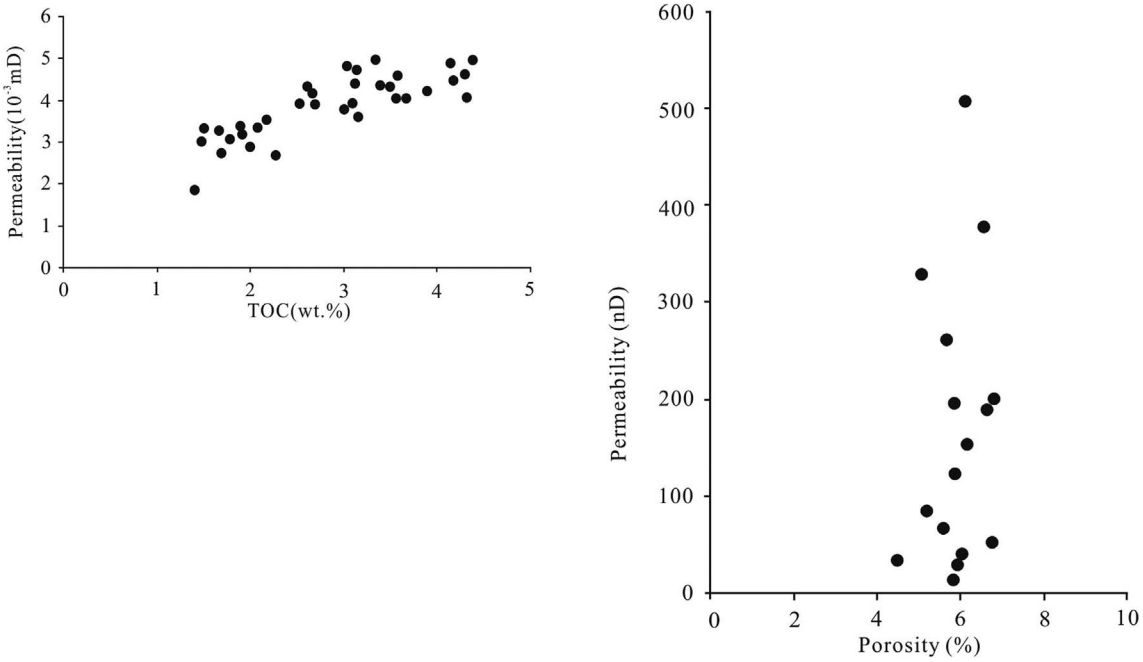

Fig. 3. Plot of TOC vs. permeability in the Duvernay Shale (modified from Dunn et al., 2012) (A). Plot of porosity vs. permeability in the Duvernay Shale (B).

porosity as well as their spatial variation in the Duvernay Shale was estimated using TOC content, hydrocarbon expulsion efficiency factor (f) derived from kerogen kinetics modeling (Chen and Jiang, 2016). For total gas storage, the shale gas-in-place volumes are generally considered in terms of adsorbed gas and free gas. This is because in current industry standard, the solution gas in mobiles hydrocarbon and water was combined with adsorbed gas within organic matter in the adsorption isotherm analysis (Ambrose et al., 2010). The absorption capacity of Duvernay Shale was assessed with TOC content, modeled pore pressure and isothermal absorption experiment (Eq. (2)). The free gas storage capacity of organic pores in the Duvernay shale was calculated with correction from the volume occupied by sorbed gas (Ambrose et al., 2010) (Eq. (3)), based on which the in-place adsorbed gas volume and free gas volume were determined, respectively (modified from Kuuskraa et al., 2013) (Eqs.(4),(5)). The in-place shale gas and oil volumes hosted by organic-pores were estimated using volumetric method (Eq. (6) -Eq. (7)).

$$\varphi_{org} = \gamma\left[C_{toc}^{o}\alpha f T_R\left(1 - \frac{0.833C_{toc}}{100}\right)\right]\frac{\rho_b}{\rho_k} \quad (1)$$

$$G_a = G_{sL}\frac{P}{P+P_L} \quad (2)$$

$$G_f = \frac{32.0368}{B_g}\left[\frac{\varnothing_{org}(1 - S_w)}{\rho_b} - \frac{1.318 \times 10^{-6}M}{\rho_s}\left(G_{sL}\frac{P}{P+P_L}\right)\right] \quad (3)$$

$$G_{in-place}^{adsorbed} = V_{rock}\rho_b\varnothing_{org}G_a \quad (4)$$

$$G_{in-place}^{free} = V_{rock}\rho_b\varnothing_{org}G_f \quad (5)$$

$$G_{in-place} = G_{in-place}^{free} + G_{in-place}^{adsorbed} \quad (6)$$

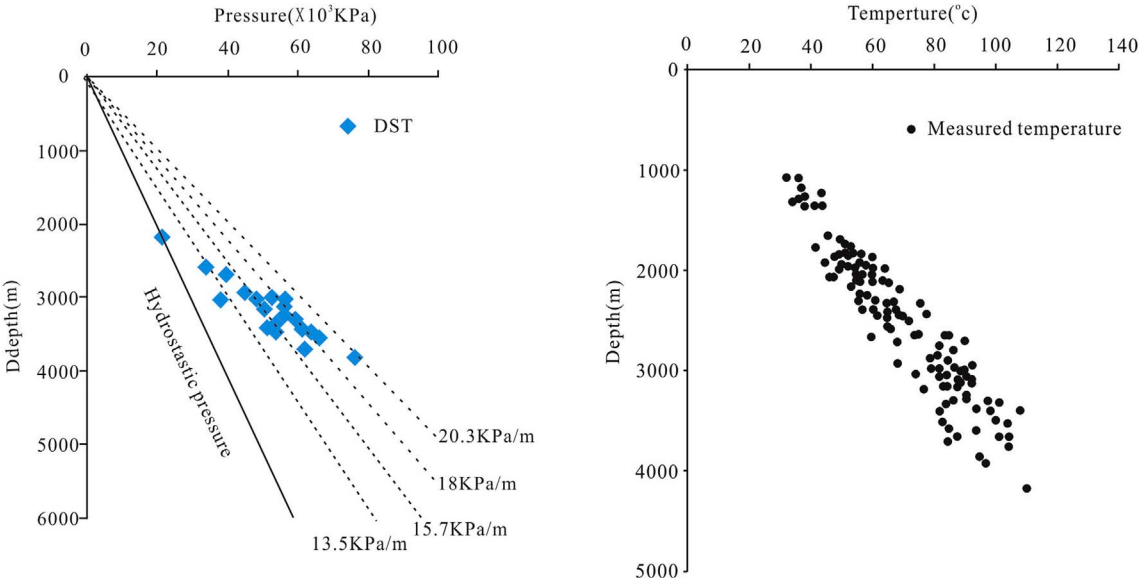

Fig. 4. Formation pressures from DSTs result of recent production wells (A). The General trends of formation temperature with depth in WCSB (B).

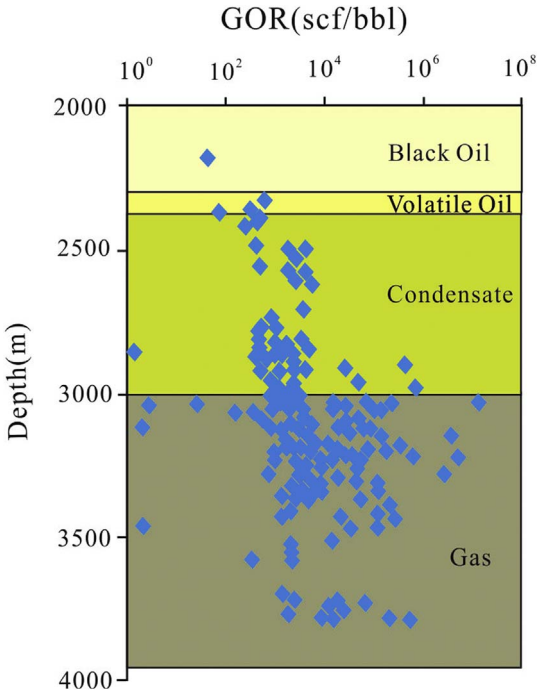

Fig. 5. GOR from first month production data indicates the variation of hydrocarbon compositions with thermal maturation in Duvernay Formation.

$$Oil_{in-place} = V_{rock}\rho_b \varnothing_{org}/B_{oi} \quad (7)$$

Where TR is the ratio of generated hydrocarbon to the total hydrocarbon generation potential; f is hydrocarbon expulsion efficiency factor; C^o_{toc} and C_{toc} are the initial TOC content and residual TOC content (wt. %); α is a scaling parameter associated with kerogen type; ρ_b and ρ_k are the bulk rock density and density of kerogen, 2.6 and 1.2 g/cm^3, respectively; ϒ is the carbon equivalent mass of kerogen in hydrocarbon conversion (ϒ = 1.2). G_a *and* G_f are absorption capacity and free gas storage capacity (scf/ton); $\varnothing_{org}$ is the organic porosity (%); S_w is the fraction of the porosity filled by water, with an assumption that organic pores are saturated with hydrocarbon, $S_w = 0$; B_g is the gas volume factor; M is the apparent natural gas molecular weight (lbm/lbmole); G_{sL} is the Langmuir storage capacity (scf/ton); P and P_L are the formation pressure and Langmuir pressure (MPa) respectively; ρ_s is sorbed gas phase density (g/cm^3), respectively. $G^{adsorbed}_{in-place}$ and $G^{free}_{in-place}$ are in-place absorption and free gas potential (TCF); $G_{in-place}$ and $Oil_{in-place}$ are total in-place gas and oil resource potential (TCF and MMbbl); B_{oi} is the oil formation gas volume factor, V_{rock} is the rock volume, m^3.

4. Results

4.1. Petroleum system

Fig. 6 shows the specific geochemical characteristics of the Duvernay Shale, including the distribution of TOCs (Fig. 6A), the general trend of hydrocarbon generation potential (HI) (Fig. 6B) as well as the relations between free hydrocarbon and thermal maturity (Fig. 6C). TOC in Duvernay Shale mainly varies from 2 wt % to 10 wt %, with an averaged value of 4.2 wt% (Fig. 6A). Due to the thermal maturation and kerogen decomposition, HI of the core samples in Duvernay Formation follows a decreasing trend with increasing Tmax (Fig. 6B), indicating an averaged initial HI (HIo) of 600 mg hydrocarbon/g TOC. Fig. 6C exhibits a relative high free hydrocarbon volume in samples with Tmax of 450 °C–480 °C. The modeled kerogen kinetics based on both Rock-Eval data (HI and Tmax) and dominated organic facies illustrate the general trend of hydrocarbon generation and expulsion in Duvernay source rock (Fig. 6D). The hydrocarbon transformation ratio versus thermal maturity (Tmax) was employed to quantify hydrocarbon generation in the Duvernay petroleum system. It appears that significant hydrocarbon generation (20% TR) began around Ro of 0.65% and terminated (95% TR) at Ro of 1.85%. Gas generation suggested by HC_{1-4} generation index significantly increased from Ro of 1.1%, and the gas expulsion (instantaneous HC_{1-4} expulsion) began shortly after the source rock entered the gas window at Ro of 1.30% and reached a peak value at Ro of 1.66%. The difference between the increasing trend of HC_{1-4} generation and the decreasing trend of HC_{1-4} expulsion may indicate a considerable retained gas in Duvernay Shale, which is consistent with the free hydrocarbon in Fig. 6C.

The primary burial history and thermal history in the 103/10-059-18W5 well (Fig. 1) are shown by a 1-D extraction from the 2-D model (Fig. 7). Sweeney and Burnham's (1990) kinetics for Ro were used to calibrate the thermal history. The burial history model illustrates decompaction through subtle increasing in layer thickness backward through time. Included in Fig. 8 are two erosions during 150 Ma to 119 Ma and 57.8 Ma to the present.

Based on general depositional and erosional trends recorded in the burial history, modeled temperature and vitrinite reflectance exhibit fairly good correlation with the measured ones (Fig. 8). For example, the measured bottom hole temperature in the 103/10–059/18W5 well is about 100°C, while the modeled temperature at 3300 m is almost the same as this temperature. The thermal history from the 103/10/059/18W5 well illustrates that the Duvernay Shale reached “oil window” about 70–80 Ma ago and the present-day Ro of 1–1.2% was achieved about 50 Ma ago (Fig. 7). Duvernay and older source rocks would be thermally mature for gas generation at this location.

Displayed in Fig. 9 is specific distribution of the modeled vitrinite reflectance, exhibiting a general good agreement with the conversed Ro from wells. The expected %Ro of primary vitrinite in the Duvernay Shale varies between 0.4% in the northeast and 2.2% in the southwest, which indicates that most part of Duvernay Shale are within hydrocarbon generation window. Also, the wide range of vitrinite reflectance (%Ro) indicates the existence of various type of hydrocarbons in Duvernay Shale, and the high vitrinite reflectance (%Ro) along the deformational front indicates a huge shale gas potential in this section.

Studies suggest that nanometer-scale organic pores are thermal maturity- and initial TOC content-dependence (Modica and Lapierre, 2012; Chen and Jiang, 2016). The organic porosity of Duvernay Shale within zone of Ro > 0.7% determined with the method proposed by Chen and Jiang (2016) varies spatially in the central Alberta with the maximum value up to 7% (Fig. 10). Since the storage space within kerogen networks dominants gas capacity of shale reservoir (Loucks et al., 2009, 2011, 2012; Modica and Lapierre, 2012; Chalmers et al., 2012; Curtis et al., 2012; Curtis, 2013; Romero-Sarmiento et al., 2014; Lu et al., 2015), locally well-developed organic pores in Duvernay Shale are favourable to develop the “sweet spots”, which can be confirmed by the production data from Hammermaster et al. (2012).

Previous studies from Marquez and Mountjoy (1996), Michael and Bachu (2001) suggested the hydrocarbon generation was responsible for the overpressure in the Duvernay Shale. Calibrating to the measured formation pressure, the modeled pressure contour indicates the pore-pressure magnitude generated by hydrocarbon generation increases from northeast towards southwest, which increases in a fast speed within the zone where the vitrinite reflectance is over 0.8% (Fig. 11). Calculated organic porosity in Fig. 10 and pore pressure in Fig. 11 generally share some similar high value zones, confirming that high pore pressure in the Duvernay shale was derived from gas generation.

4.2. Absorption capacity and free gas capacity

A critical parameter for shale gas reservoir evaluation is the gas adsorption capacity. About 5 adsorption isothermals measured by Beaton et al. (2010) were used to characterize the variation of adsorption capacity as a function of TOC content, thermal maturity

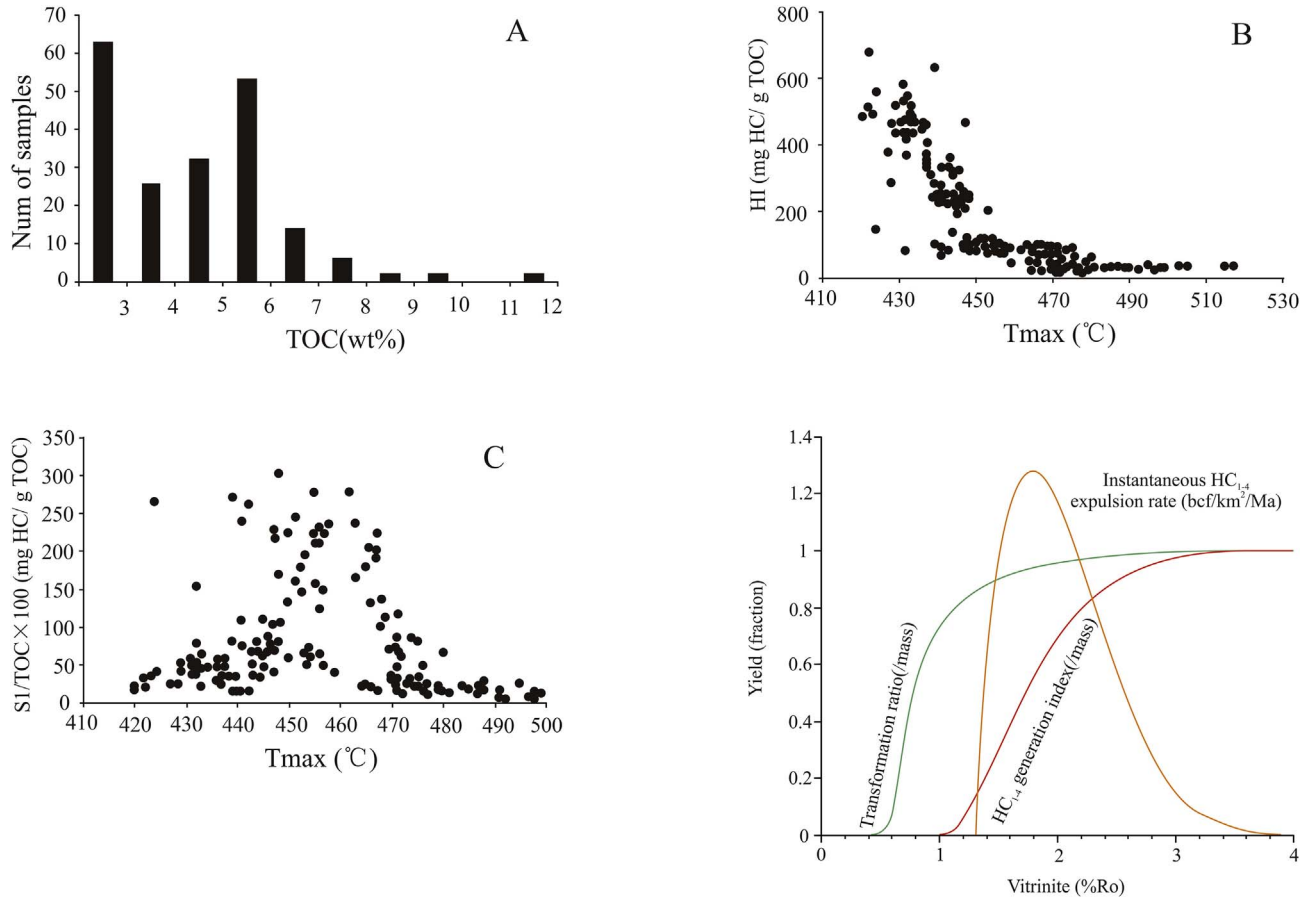

Fig. 6. Diagrams showing Rock-Eval data of core samples from the Duvernay Formation in WCSB. The distribution of present-day total organic carbon (TOC) content in the rock samples (A). The remaining hydrocarbon generation potential (HI) (B). The amount of free hydrocarbon in samples (S_1/TOC × 100, mg HC/g TOC) as a function of thermal maturity (C). The kerogen kinetics model of the Duvernay Shale assigned with averaged TOC value of 4.2 wt%, initial HI value of 600 mg HC/g TOC (D). The Tmax on X-axis was conversed from vitrinite reflectance (%Ro) with a modified empirical formula from Wust et al. (2013): Tmax = (Ro + 10.10)/0.024.

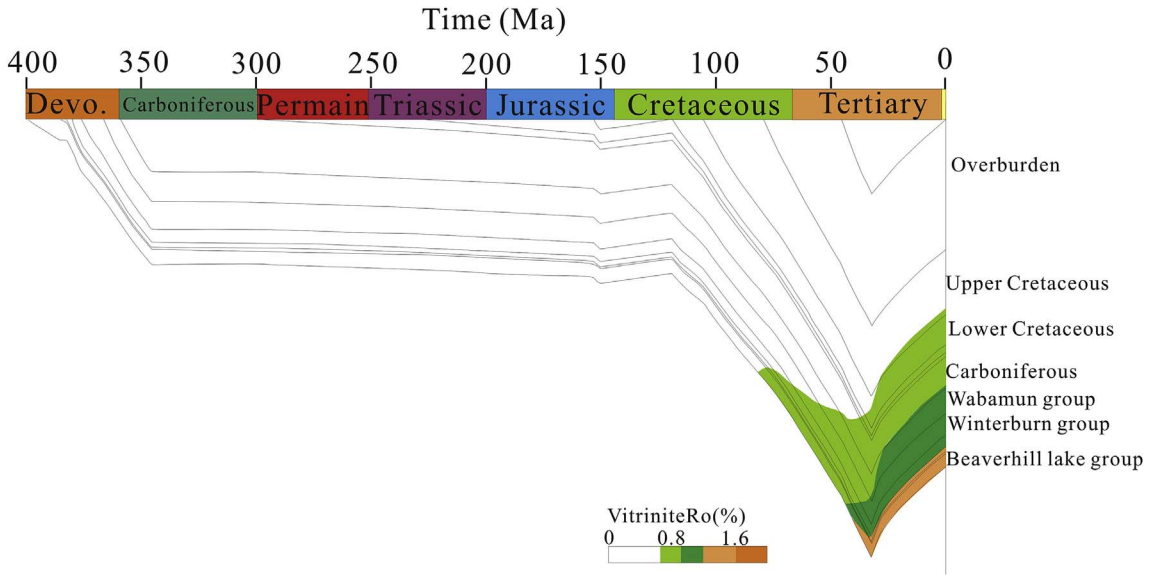

Fig. 7. The thermal history based on a 1-D extraction of the 103/10/059/18W5 well from the 2-D model. The kinetics for Ro proposed by Sweeney and Burnham (1990) were used to calibrate the thermal history.

(Tmax), pressure and temperature (Ross and Bustin, 2008) of the Duvernay Shale. As Fig. 12 exhibits, gas adsorption capacity varies significantly as a function of TOC, thermal maturity, temperature and pressure. Specifically, the Langmuir volume, describing the maximum volume of gas absorbed onto surface area, linearly increases with organic matter content in Duvernay shale (Fig. 13), since organic matter can provide large specific surface area and sorption sites (Hickey and Henk, 2007; Ross and Bustin, 2008). The modeled adsorption capacity

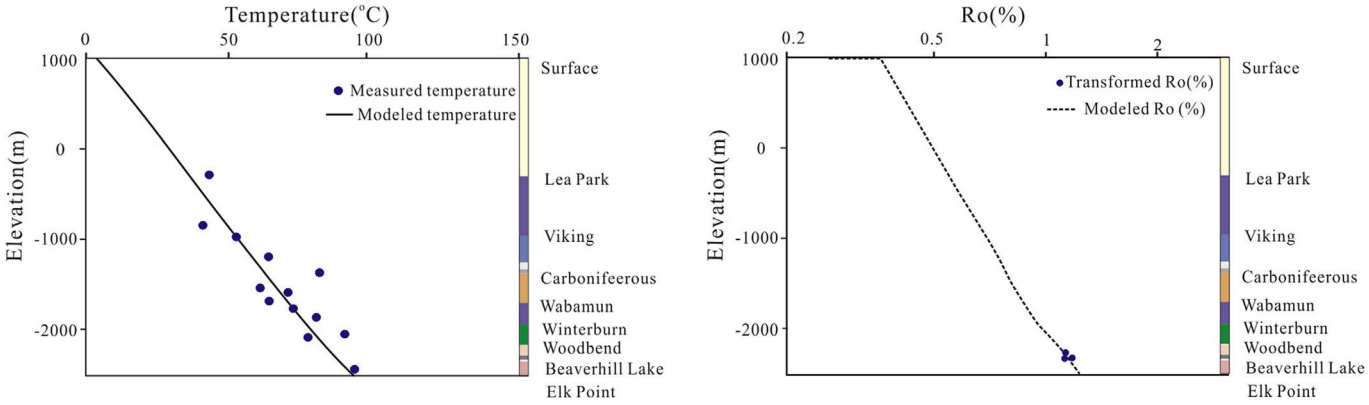

Fig. 8. Comparison of modeled and measured present day temperature and Ro% of the 103/10-059-18w5 well.

of Duvernay Shale determined with Eq. (1) ranges from 8 to 30 scf/ton in WCSB.

Studies indicate that nano-metre scale pores typically determine free gas capacity in self-contained source-reservoir shale system (Loucks et al., 2012; Romero-Sarmiento et al., 2014). The free gas capacity in organic pores of Duvernay Shale determined with Eq. (2) indicates that free gas capacity ranges from 40 to 140 scf/ton. Compared with the absorption capacity, free gas phase plays a more significant role of the total gas-in-place in Duvernay Shale.

4.3. In-place shale oil and gas potential

The adsorbed gas in-place (GIP) and free gas GIP in the Duvernay Shale are calculated with Eq. (3) and Eq. (4) in dry gas and wet gas zones in Fig. 9 defined by vitrinite reflectance > 1.1%. And the shale gas resource potential was determined with Eq. (5) (see Table 1). As a result, the averaged absorbed gas and free gas volume determined by volumetric method is 58.2 and 346.6 TCF, respectively, which means, the estimated averaged total natural gas in-place is 404.8 TCF in Duvernay shale. The median value of in-place shale oil resource determined with Eq. (6), including condensate and volatile oil in prospective area, is about 81,420 MMbbl.

5. Discussion

Due to abundant specific surface areas and sorption sites from organic matter, TOC has been typically regarded as the primary controlling factor for sorption capacity in marine shale around the world (Lu et al., 1995; Chalmers and Bustin, 2008; Gasparik et al., 2014; Ross and Bustin, 2009; Tan, 2014; Wang et al., 2013, 2016). Besides the occurrence of organic matter, previous studies from Gasparik et al. (2014), Ross and Bustin (2009) suggested that mineral compositions, especially clay minerals, also made a great contribution to the sorption capacity. Specifically, illite, kaolinite, and interbedded illite-smectite,

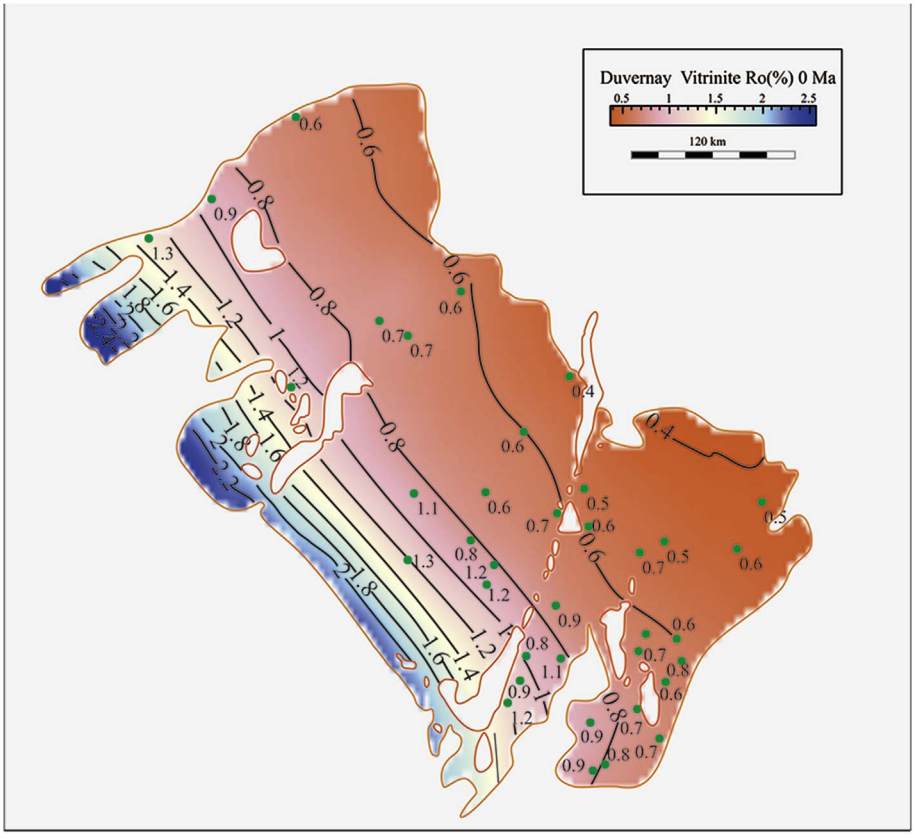

Fig. 9. Modeled thermal maturity (% Ro) contour map of the Duvernay Shale, WCSB.

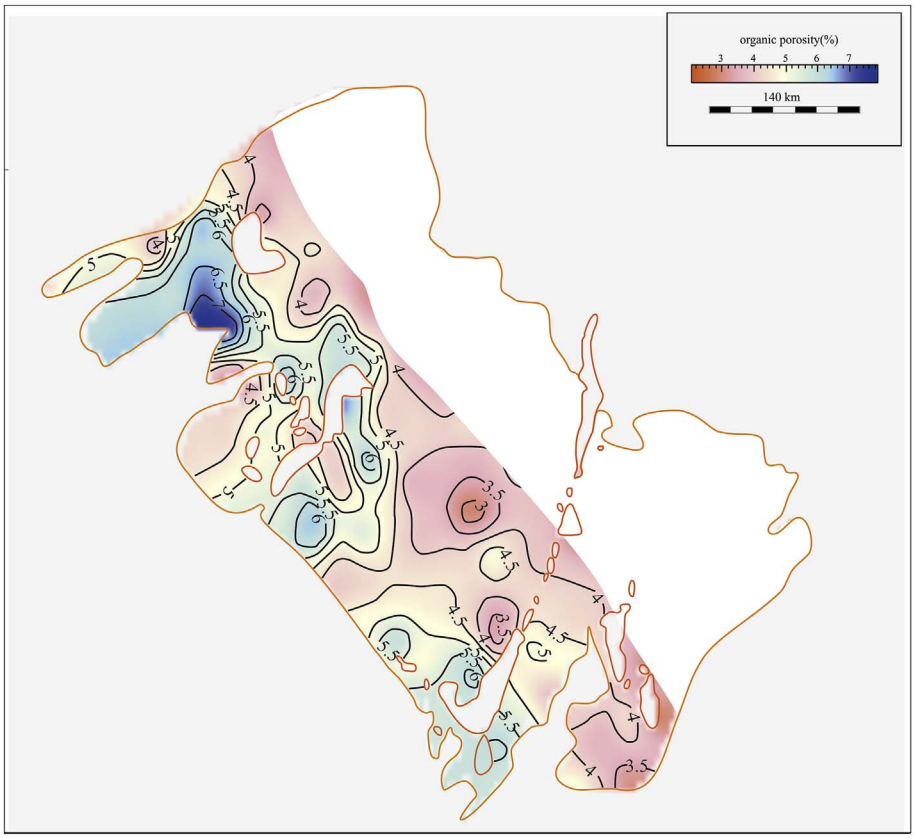

Fig. 10. Calculated organic porosity contour map of the Duvernay Shale.

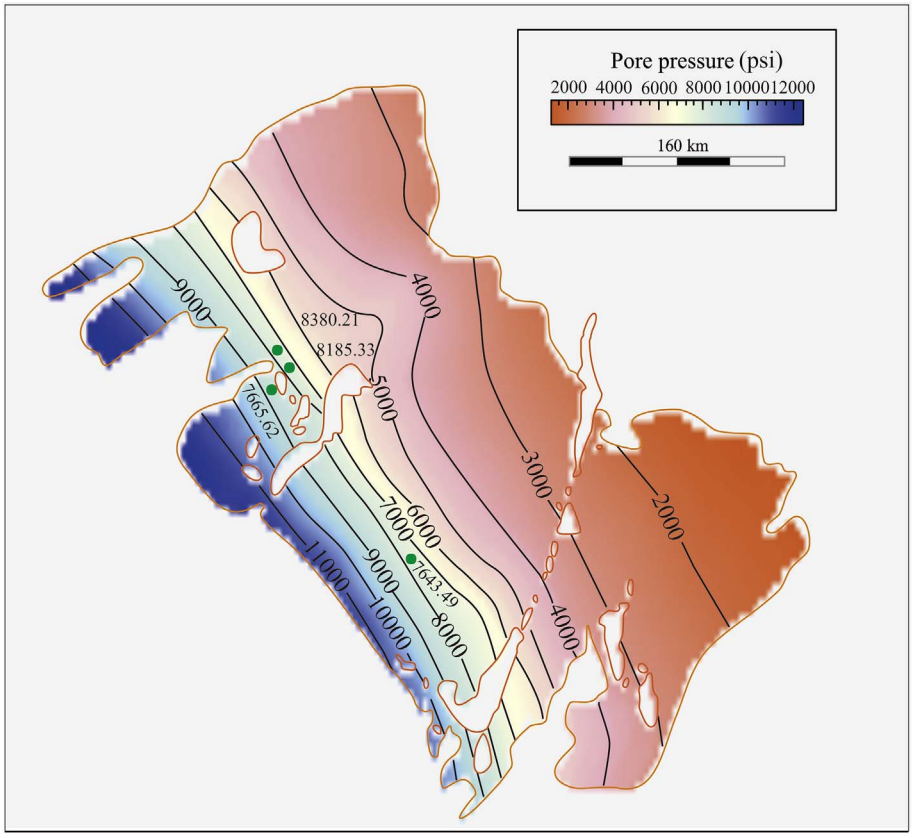

Fig. 11. Modeled pore pressure contour map of the Duvernay Shale.

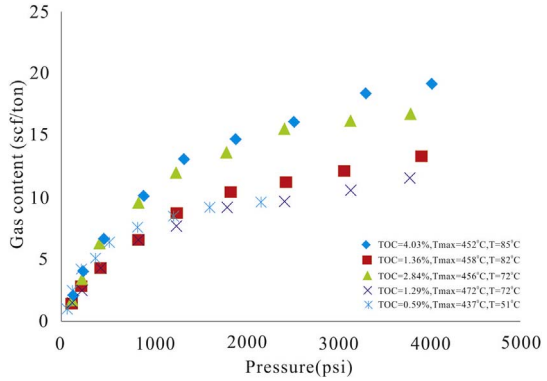

Fig. 12. Adsorption isotherms of 5 samples from the Dvuernay Shale (According to Beaton et al., 2010).

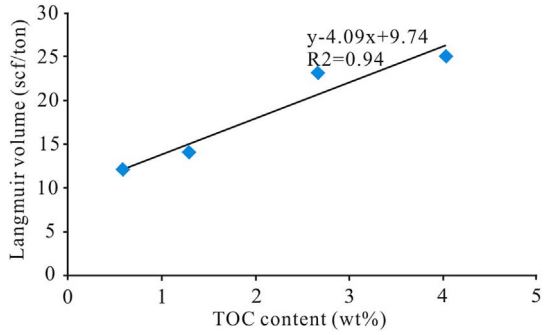

Fig. 13. The Langmuir volume vs. TOC content plot showing the Langmuir volume increase substantially with the TOC content in Duvernay Shale.

etc., could provide certain adsorption sites for natural gas due to the small pore sizes they formed. Also, study from Zhang et al. (2012) indicated that nano-pore volume generally increased with thermal maturity, which could enhance the adsorption capacity as well. However, the adsorption capacity in this study was assumed to be controlled by TOC content, and formation pressure and temperature without considering the mineral compositions and thermal maturity, which was based on following reasons. Empirical data shows a good correlation between TOC and Langmuir maximum adsorption capacity in shale gas plays with $R^2 > 0.98$ for shale samples from various sources (Zhang et al., 2012), $R^2 = 0.97$ for samples from the Marcellus Shale and $R^2 = 0.94$ for Duvernay Shale in this study, which means, TOC explains > 94% variation in the maximum adsorption capacity in general for Duvernay Shale. Water could substantially reduce the adsorption capacity by pre-occupying the pore-surface of clay minerals and eliminate the amount of methane in sorption phase by restricting the access to active sites, since clay minerals were typically saturated with water during deposition, which can form an irreducible film on the surface of clay minerals (Zhang et al., 2012). The source of methane is another obstacle for large amount of methane being adsorbed on mineral surfaces. Since hydrocarbon generation and primary migration initially take place within kerogen network in general, only those in close contact with the kerogen network or primary migration routes have a chance to receive methane gas.

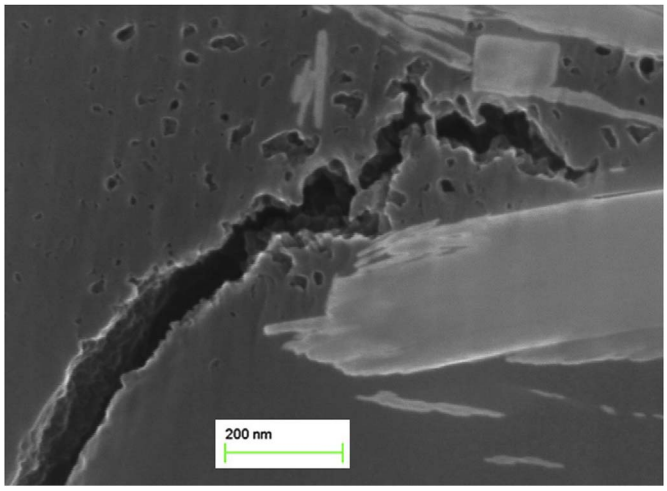

Fig. 14. SEM images showing fracture and organic pores in organic matter, Duvernay Shale, WCSB.

Totally 3 types of pores generally exist in shale oil and gas system, including organic pores derived from decomposition of organic matter, matrix pores, and fractures (Jarvie, 2012). Jarvie (2012) and Gale et al. (2014) confirmed that considerable open fractures existed in shale reservoir, while one such unconventional shale gas system was the Monterey Shale. Natural fractures in low-matrix-permeability shale reservoir may play an important role in fluid flow and contribute greatly to the shale gas storage potential as well, since a significant fraction of shale gas may be stored as free gas in natural fractures (Curtis, 2002; Jarvie et al., 2003; Gale et al., 2014). For example, SEM image in Fig. 14 exhibits well-developed fracture within the Duverney Formation. Compared with nano-pores with pore diameter less than hundreds nm, these fractures with width larger than 1 mm appear to be more significant for fluid flow and free-gas storage in shale reservoirs. Unfortunately, the impacts of fractures in petroleum system and shale gas assessment remain a discussion open to the future research.

6. Conclusion

1. Duvernay Shale reached “oil window” and “gas window” about 70–80 Ma ago and 50 Ma ago, respectively. Significant hydrocarbon generation (20% TR) began around Ro of 0.65% and terminated (95% TR) at Ro of 1.85%. Gas generation rates increased dramatically from Ro of 1.1%, while the instantaneous HC_{1-4} expulsion reached peak at Ro of 1.66%. The difference between the HC_{1-4} generation curve and the HC_{1-4} expulsion curve indicates a considerable retained gas in Duvernay Shale.
2. High organic matter content (an averaged TOC value of 4.2 wt%) and wide gas generation window (Tmax ranging from 465 °C to 526 °C) indicates considerable organic pores associated with the conversion of solid kerogen to hydrocarbon in Duvernay Shale. And the calculated organic porosity can be up to 7% with a medium value of 4.5%.
3. Varying primarily as a function of organic matter and formation

Table 1
Summary of parameters used to assess shale-hosted hydrocarbon resource of the Duvernay Shale.

	Area	Averaged thickness	Rock density	Organic porosity	Averaged Bg	Averaged Boi
	(km^2)	(m)	kg/m^3	%		
adsorbed gas	14485	50	2600	6		
free gas	14485	50	2600	6	0.0029	
oil	18580.5	50	2600	6		1.78

pressure, the absorption capacity of the Duvernay Shale ranges from 8 to 30 scf/ton, while the free gas capacity ranges from 40 to 140 scf/ton. The estimated median value of total in-place natural gas and in-place shale oil resource in organic pores of Duvernay shale are 404.8 TCF and 81420 MMbbl, indicating a significantly shale oil and gas resource target in WCSB.

Acknowledgements

We are grateful to Yoho Energy Limited for providing the laboratory test and production data of the 14-16-62-21w5 well. We would like to thank Natural Resource Canada's Geoscience for New Energy Supply (GNES) program for financial support and Geological Survey of Canada for permission to present the study result. We are grateful to the JNGSE Editor and three anonymous reviewers for their constructive comments and suggestions.

References

Allan, J., Creaney, S., 1991. Oil families of the western Canada basin. Bull. Can. Petroleum Geol. 39, 107–122.
Ambrose, R.J., Hartman, R.C., Diaz Campos, M., Akkutlu, I.Y., Sondergeld, C., 2010. New pore-scale considerations for shale gas in place calculations. In: SPE Unconventional Gas Conference. Society of Petroleum Engineer.
Anderson, S.D.A., Rokosh, C.D., Pawlowicz, J.G., Berhane, H., Beaton, A.P., 2010. Mineralogy, Permeametry, Mercury Porosimetry, Pycnometry and Scanning Electron Microscope Imaging of Duvernay and Muskwa Formations in Alberta: Shale Gas Data Release. ERCB/AGS Open File Report 2010–02.
Beaton, A.P., Pawlowicz, J.G., Anderson, S.D.A., Berhane, H., Rokosh, C.D., 2010. In: Rock Eval™, Total Organic Carbon and Adsorption Isotherms of the Duvernay and Muskwa Formations in Alberta: Shale Gas Data Release, ERCB/AGS Open File Report.
Chalmers, G.R., Bustin, R.M., 2008. Lower Cretaceous gas shales in northeastern British Columbia, Part I: geological controls on methane sorption capacity. Bull. Can. petroleum Geol. 56 (1), 1–21.
Chalmers, G.R., Bustin, R.M., Power, I.M., 2012. Characterization of gas shale pore systems by porosimetry, pycnometry, surface area, and field emission scanning electron microscopy/transmission electron microscopy image analyses: examples from the Barnett, Woodford, Haynesville, Marcellus, and Doig units. AAPG Bull. 96 (6), 1099–1119.
Chen, Z., Jiang, C., 2016. A revised method for organic porosity estimation using Rock-Eval pyrolysis data, example from Duvernay Shale in the Western Canada Sedimentary Basin. AAPG Bull. 100, 405–422.
Chow, N., Wendte, J., Stasiuk, L.D., 1995. Productivity versus preservation controls on two organic-rich carbonate facies in the Devonian of Alberta: sedimentological and organic petrological evidence. Bull. Can. Petroleum Geol. 43, 433–460.
Curtis, J.B., 2002. Fractured shale-gas systems. AAPG Bull. 86 (11), 1921–1938.
Curtis, M.E., 2013. Influence of thermal maturity on organic shale microstructure; Oklahoma shale gas and oil workshop, november 20, 2013. Last access: June 12, 2014. http://www.ogs.ou.edu/MEETINGS/Presentations/2013Shale/2013ShaleCurtis.pdf.
Curtis, M.E., Cardott, B.J., Sondergeld, C.H., Rai, C.S., 2012. Development of organic porosity in the Woodford Shale with increasing thermal maturity. Int. J. Coal Geol. 103, 26–31.
Ducros, M., Euzen, T., Vially, R., Sassi, W., 2012. 2-D Basin Modeling of the WCSB across the Montney-doig System: Implications for Hydrocarbon Migration Pathways and Unconventional Resources Potential. GeoConvention 2014: FOCUS.
Dunn, L., Schmidt, G., Hammermaster, K., Brown, M., Bernard, R., Wen, E., Befus, R., Gardiner, S., 2012. The Duvernay Formation (Devonian) Sedimentology and Reservoir Characterization of a Shale Gas Liquids Play in Alberta, Canada.
Gale, J.F., Laubach, S.E., Olson, J.E., Eichhubl, P., Fall, A., 2014. Natural fractures in shale: a review and new observations. AAPG Bull. 98 (11), 2165–2216.
Gasparik, M., Bertier, P., Gensterblum, Y., Ghanizadeh, A., Krooss, B.M., Littke, R., 2014. Geological controls on the methane storage capacity in organic-rich shales. Int. J. Coal Geol. 123, 34–51.
Hammermaster, K., Schmidt, G., Dunn, L., Brown, M., Bernard, R., Wen, E., Befus, R., Gardiner, S., 2012. The Duvernay Formation (Devonian): an emerging shale liquids play in Alberta. In: Canadian Society of Petroleum Geologists. Annual Convention, Calgary.
Higley, D.K., Lewan, M.D., Roberts, L.N., Henry, M., 2009. Timing and petroleum sources for the Lower Cretaceous Mannville Group oil sands of northern Alberta based on 4-D modeling. AAPG Bull. 93 (2), 203–230.
Hickey, J.J., Henk, B., 2007. Lithofacies summary of the mississippian barnett shale, mitchell 2 TP sims well, wise county, Texas. AAPG Bull. 91 (4), 437–443.
Jarvie, D.M., 2012. Shale resource systems for oil and gas: part 1—shale-gas resource systems. In: In: Breyer, J.A. (Ed.), Shale Reservoirs—Giant Resources for the 21st Century 97. AAPG Memoir, pp. 69–87.
Jarvie, D.M., Hill, R.J., Pollastro, R.M., Wavrek, D.A., Claxton, B.L., Tobey, M.H., 2003. Evaluation of unconventional natural gas prospects: the Barnett Shale fractured shale gas model. In: Proceedings of European Association of International Organic Geochemists Meeting, pp. 60–70.
Ko, L.T., Loucks, R.G., Zhang, T., Ruppel, S.C., Shao, D., 2016. Pore and pore network evolution of Upper Cretaceous Boquillas (Eagle Ford–equivalent) mudrocks: results from gold tube pyrolysis experiments. AAPG Bull. 100 (11), 1693–1722.
Kuuskraa, V.A., Stevens, S., Moodhe, K., 2013. World shale gas and shale oil resources assessment. 2013-06-17 [2016-05-09]. http://www.eia.gov/conference/2013/pdf/presentations/kuuskraa.pdf.
Loucks, R.G., Ruppel, S., Reed, R.M., Hammes, U., Zahm, C., 2011. Origin and classification of pores in mudstones from shale-gas systems. Search Discov. Article 40855, 1–32.
Loucks, R.G., Reed, R.M., Ruppel, S.C., Jarvie, D.M., 2009. Morphology, genesis, and distribution of nanometer-scale pores in siliceous mudstones of the Mississippian Barnett Shale. J. Sediment. Res. 79 (12), 848–861.
Loucks, R.G., Reed, R.M., Ruppel, S.C., Hammes, U., 2012. Spectrum of pore types and networks in mudrocks and a descriptive classification for matrix-related mudrock pores. AAPG Bull. 96 (6), 1071–1098.
Low, W.S., Kennedy, J., Fisher, G., Greene, M., 2013. The Duvernay shale: the new millennium gold is condensate. https://datarooms.ca.bmo.com/Login%20Page%20Document%20Library/ADLibrary/ADDrillBits/AD%20Drill%20Bits%20Duvernay%20Shale%20November%202013.pdf.
Lu, J., Ruppel, S.C., Rowe, H.D., 2015. Organic matter pores and oil generation in the Tuscaloosa marine shale. AAPG Bull. 99 (2), 333–357.
Lu, X.C., Li, F.C., Watson, A.T., 1995. Adsorption measurements in Devonian shales. Fuel 74, 599–603.
Marquez, X.M., Mountjoy, E.W., 1996. Microfractures due to overpressures caused by thermal cracking in well-sealed Upper Devonian reservoirs, deep Alberta Basin. AAPG Bull. 80 (4), 570–588.
Michael, K., Bachu, S., 2001. Fluids and pressure distributions in the foreland-basin succession in the west-central part of the Alberta Basin, Canada: evidence for permeability barriers and hydrocarbon generation and migration. AAPG Bull. 85 (7), 1231–1252.
Modica, C.J., Lapierre, S.G., 2012. Estimation of kerogen porosity in source rocks as a function of thermal transformation: example from the Mowry Shale in the Powder River Basin of Wyoming. AAPG Bull. 96, 87–108.
Mossop, G., Shetsen, I., 1994. Geological atlas of the western Canada Sedimentary Basin. Published jointly by the canadian society of petroleum geologists and the Alberta research council. In: Sponsorship Association with the Alberta Department of Energy and the Geological Survey of Canada, pp. 126–127.
Peters, K.E., 1986. Guidelines for evaluating petroleum source rock using programmed pyrolysis. AAPG Bull. 70, 318–329.
Pommer, M., Milliken, K., 2015. Pore types and pore-size distributions across thermal maturity, Eagle Ford Formation, southern Texas. AAPG Bull. 99 (9), 1713–1744.
Rokosh, C.D., Lyster, S., Anderson, S.D.A., Beaton, A.P., Berhane, H., Brazzoni, T., Chen, D., Cheng, Y., Mack, T., Pana, C., Pawlowicz, J.G., 2012. Summary of Alberta's Shale- and Siltstone-hosted Hydrocarbon Resource Potential. ERCB/AGS Open File Report. 8. .
Romero-Sarmiento, M.F., Ducros, M., Carpentier, B., Lorant, F., Cacas, M.C., Pegaz-Fiornet, S., Wolf, S., Moretti, I., 2013. Quantitative evaluation of TOC, organic porosity and gas retention distribution in a gas shale play using petroleum system modeling: application to the Mississippian Barnett Shale. Mar. Petroleum Geol. 45, 315–330.
Romero-Sarmiento, M.F., Rouzaud, J.N., Bernard, S., Deldicque, D., Thomas, M., Littke, R., 2014. Evolution of Barnett Shale organic carbon structure and nanostructure with increasing maturation. Org. Geochem. 71, 7–16.
Ross, D.J.K., Bustin, R.M., 2007. Shale gas potential of the lower jurassic gordondale member, northeastern british columbia, Canada. Bull. Can. Petroleum Geol. 55, 51–75.
Ross, D.J., Bustin, R.M., 2008. Characterizing the shale gas resource potential of Devonian–Mississippian strata in the Western Canada sedimentary basin: application of an integrated formation evaluation. AAPG Bull. 92 (1), 87–125.
Ross, D.J., Bustin, R.M., 2009. The importance of shale composition and pore structure upon gas storage potential of shale gas reservoirs. Mar. Petroleum Geol. 26 (6), 916–927.
Stasiuk, L.D., Fowler, M.G., 2004. Organic facies in Devonian and Mississippian strata of Western Canada Sedimentary Basin: relation to kerogen type, paleoenvironment, and paleogeography. Bull. Can. Petroleum Geol. 52 (3), 234–255.
Stasiuk, L.D., Fowler, M.G., 2002. Thermal maturity Evaluation (Vitrinite and Vitrinite Reflectance Equivalent) of Middle Devonian, Upper Devonian, and Mississippian Strata in the Western Canada Sedimentary Basin: Geological Survey of Canada. Open File 4341 (CD-ROM).
Stoakes, F.A., Creaney, S., 1984. Sedimentology of acarbonate source rock: duvernay Formation of central Alberta. In: Eliuk, L. (Ed.), Carbonates in Subsurface and Outcrop: Proceedings of the 1984 Canadian Society of Petroleum Geologists Core Conference, Calgary, Alberta, Canada, pp. 132–147.
Sweeney, J.J., Burnham, A.K., 1990. Evaluation of a simple model of vitrinite reflectance based on chemical kinetics. AAPG Bull. 74, 1559–1570.
Tan, J., 2014. Shale Gas Potential of the Major Marine Shale Formations in the Upper Yangtze Platform, South China. Doctoral dissertation. TechnischeUniversität Berlin.
Wang, S., Song, Z., Cao, T., Song, X., 2013. The methane sorption capacity of Paleozoic shales from the Sichuan Basin, China. Mar. Petroleum Geol. 44, 112–119.
Wang, P., Chen, Z., Pang, X., Hu, K., Sun, M., Chen, X., 2016. Revised models for determining toc in shale play: example from devonian duvernay shale, western Canada sedimentary basin. Mar. Petroleum Geol. 70, 304–319.
Wust, R.A., Nassichuk, B.R., Brezovski, R., Hackley, P.C., Willment, N., 2013. Vitrinite reflectance versus pyrolysis Tmax data: assessing thermal maturity in shale plays with special reference to the Duvernay shale play of the Western Canadian Sedimentary Basin, Alberta, Canada. In: SPE Unconventional Resources Conference and Exhibition-asia Pacific. Society of Petroleum Engineers.
Zhang, T., Ellis, G.S., Ruppel, S.C., Milliken, K., Yang, R., 2012. Effect of organic-matter type and thermal maturity on methane adsorption in shale-gas systems. Org. Geochem. 47, 120–131.